Investigation of MC3T3-E1 Cell Behavior on the Surface of GRGDS-Coupled Chitosan

Jing Li, Huan Yun, Yandao Gong, Nanming Zhao, and Xiufang Zhang*

Department of Biological Sciences and Biotechnology, State Key Laboratory of Biomembrane and Membrane Biotechnology, Tsinghua University, Beijing 100084, P. R. China

Received November 29, 2005; Revised Manuscript Received February 20, 2006

The GRGDS (Gly-Arg-Gly-Asp-Ser) peptide has intermediate affinity to $\alpha_V\beta_3$ and $\alpha_{IIb}\beta_3$, which are the integrins most reported to be involved in bone function. In this study, biomimetic chitosan films modified with GRGDS peptide were prepared and were used as a substrate for the in vitro culture of MC3T3-E1 cells in order to investigate the effect of GRGDS modification on MC3T3-E1 cell behavior. The results of electron spectroscopy for chemical analysis (ESCA), attenuated total reflection-Fourier transform infrared spectra (ATR-FTIR), and amino acid analysis (AAA) demonstrated that the chitosan films were successfully modified with GRGDS peptides and that the surface density of the immobilized GRGDS was on the order of 10^{-9} mol/cm^2. The immobilization of the GRGDS sequence on chitosan as well as the peptide concentration play a significant role in MC3T3-E1 cell behavior. MC3T3-E1 cell attachment, proliferation, migration, differentiation, and mineralization were remarkably greater on GRGDS-coupled chitosan than on unmodified chitosan. Besides, the degree of acceleration of these biological processes was found to be dependent on peptide density. Competitive inhibition of MC3T3-E1 cell attachment using soluble GRGDS peptides indicated that the interaction of MC3T3-E1 cells with the surface of the materials was ligand-specific. Cytoskeleton organization in the fully spread MC3T3-E1 cells was highly obvious on GRGDS-coupled chitosan when compared to the lack of actin fibers noted in the round MC3T3-E1 cells on unmodified chitosan. These results suggest that MC3T3-E1 cell function can be modulated, in a peptide density-dependent manner, by the immolization of GRGDS peptide on chitosan used for scaffold-based bone tissue engineering.

Introduction

Although bone tissue possesses the capacity for regenerative growth, the bone repair process is impaired in many clinical and pathological situations.[1] For example, massive bone loss caused by trauma and tumor resection, as well as deformities, requires reconstructive surgery. While an autologous or allogenous bone graft is currently considered a standard treatment, this procedure still has many limitations.[2,3] For instance, bone grafting requires a second surgical site, where graft material is limited in quantity, and is restricted with regard to the integration of implanted bone and vascular structures with native tissue. Therefore, there is a crucial need to develop tissue engineering technologies to promote bone healing. Generally, bone tissue engineering requires identification of a suitable osteoconductive matrix that may be designed to include the release of osteoinductive factors or the delivery of osteoprogenitor cells.[4,5]

A number of extracellular matrix (ECM) proteins such as fibronectin, vitronectin, and laminin that contain the cell-binding domain RGD (Arg-Gly-Asp) have been shown to play a critical role in cell behavior, because they regulate gene expression by signal transduction set in motion by cell adhesion to the biomaterial.[6,7] The GRGDS sequence is a very intriguing member of RGD family. $\alpha_V\beta_3$, $\alpha_V\beta_5$, and $\alpha_{IIb}\beta_3$ are the integrins most reported to be involved in bone function.[8] The GRGDS peptide has been shown to have comparable affinity to $\alpha_V\beta_3$ and $\alpha_{IIb}\beta_3$ at an intermediate level and may be useful if no particular integrin is to be addressed for cell adhesion.[9] It is also reported that GRGDS plays an essential role in adhesion, remodeling, and osseointegration at the interface between a biomaterial and bone.[10] Therefore, the GRGDS sequence was chosen to modify the surface of chitosan in this study.

Chitosan (CHI) is a natural biopolymer produced by alkaline N-deacetylation of chitin, which is a natural polysaccharide occurring widely in the exoskeletons of many crustaceans and in the cell walls of some fungi. Chitosan is an interesting biomaterial due to its biocompatibility, biodegradability, mechanical properties, processability, and low toxicity. Chitosan has been used extensively in a wide range of applications, including drug carriers, wound-healing agents, chelating agents, membrane filters for water treatment, and nerve regeneration conduits.[11−15] Moreover, chitosan scaffolds are osteoconductive and can enhance bone formation both in vitro and in vivo.[16]

Chitosan can be easily modified due to the abundance of active groups, such as amino and hydroxyl groups, on the main chain. Many derivatives of chitosan can be prepared by chemical and physical modification, allowing for diverse new biological properties. Many techniques for the modification of chitosan have been attempted, including cross-linking,[17] blending,[18] grafting,[19] and irradiation by γ-ray.[20] A great deal of progress has resulted from these techniques: The capability of materials has been enhanced to a large extent, chitosan has been endowed with new characteristics, and thus, the application of chitosan has been extended. The combination of the GRGDS sequence and chitosan may be beneficial to the culture of osteoblasts.

Several studies have attempted to immobilize specific sequences that can promote cell adhesion on chitosan.[21,22] It is reported that GRGD can be photochemically grafted to *N*-succinimidyl-6-[4-azido-2-nitrophenylamino]-hexanoate (SANPAH).[21] The resulting compound can then be grafted to chitosan surfaces by subsequent ultraviolet (UV) irradiation to induce photore-

* Corresponding author. Tel: +86-10-6278-3261. Fax: +86-10-6279-4214. E-mail: zxf-dbs@mail.tsinghua.edu.cn.

10.1021/bm050913r CCC: $33.50 © 2006 American Chemical Society
Published on Web 03/21/2006

Scheme 1. Illustration of Chitosan Surface Modification Procedure

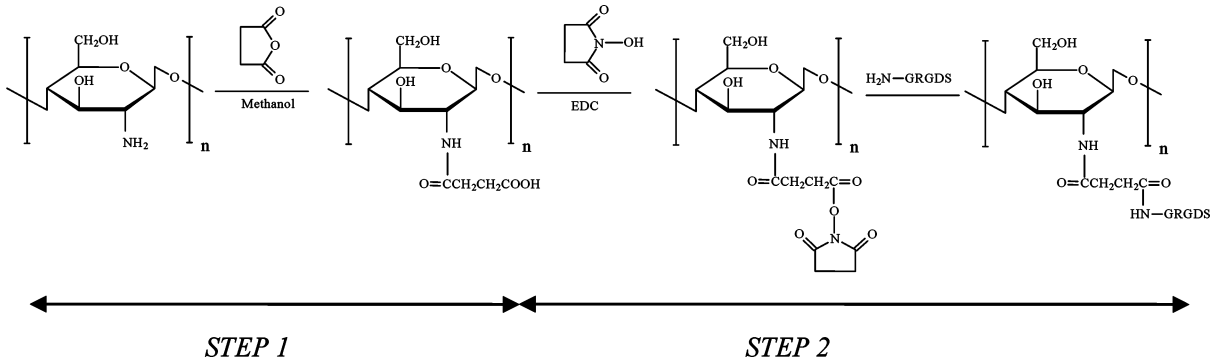

action. The modified surface leads to improved adhesion and growth of human umbilical vein endothelial cells (HUVECs).

This study focuses on the imide bond-forming reaction between chitosan and the GRGDS sequence. It is very essential for cell attachment to put a certain minimum spacing between the RGD sequence and the anchoring moiety.[23−25] Similar to the presentation of the RGD sequence in an exposed loop of a protein,[26] the RGD peptide must stand out from an artificial surface in order to reach the binding site of the integrin. Therefore, succinic anhydride was used to generate surface carboxyl groups, which can react with GRGDS peptides to form a short four-carbon arm between the GRGDS sequence and chitosan.

This study investigates the immobilization of the GRGDS sequence on chitosan surfaces through a short four-carbon arm, as well as the modulation of MC3T3-E1 cell behavior on GRGDS-coupled chitosan. The MC3T3-E1 cell, a nontransformed murine cell line derived from neonatal mouse calvaria, has been widely used as a model osteoprogenitor cell in bone tissue engineering. This study also answers the following questions: (1) Can the GRGDS sequence be successfully immobilized on the chitosan surface through a four-carbon arm? (2) Does the GRGDS-coupled chitosan provide a substrate to mediate a specific binding with MC3T3-E1 cells in a concentration-dependent manner? (3) Does peptide concentration affect cell proliferation and migration on the GRGDS-coupled chitosan? (4) Does GRGDS modification affect the actin cytoskeletal organization of MC3T3-E1 cells? (5) Does varying the peptide concentration control the differentiation and mineralization of MC3T3-E1 cells on the GRGDS-coupled chitosan?

Experimental Section

Materials. Chitosan derived from crab shell with a deacetylation degree greater than 85%, GRGDS with a FW of 490.5, *N*-hydroxysuccinimide (NHS) with a FW of 115.09, and 1-ethyl-3-(3-dimethylaminopropyl) carbodiimide (EDC) with a FW of 191.7 were all purchased from Sigma. 2-Morpholinoethanesulfonic acid (MES) with a FW of 213.2 was obtained from Amresco. Rhodamine phalloidin was acquired from Molecular Probes (Eugene, OR). Tissue culture clusters and flasks were purchased from Costar. Tissue culture plates (35 mm) were purchased from Corning. Dulbecco's minimum essential medium (DMEM) was purchased from Hyclone. Fetal bovine serum (FBS) was obtained from Hangzhou Sijiqing. All other reagents were local products of analytical grade.

Immobilization of GRGDS Peptide on the Surface of Chitosan. Chitosan (1 g) was dissolved in 100 mL of 1.2% (v/v) acetic acid solution. After stirring, the solution was filtered through a middle-pore-size nylon cloth to remove any insoluble substances. The chitosan solution was injected into the wells of tissue culture clusters, and the solvent was allowed to evaporate at 50 °C for 24 h. Then, the chitosan films were prepared.

The surface modification of chitosan films with GRGDS peptide was achieved in two steps as illustrated in Scheme 1.

Step 1. the chitosan surface was treated with succinic anhydride to generate surface carboxyl groups, which can react with the GRGDS peptide to form a short four-carbon arm. Briefly, 1% succinic anhydride in methanol solution was poured into 24-well tissue culture clusters and 35-mm tissue culture plates precoated with chitosan. The clusters were then incubated at room temperature for 7 h. After the supernatant was removed, the unreacted amino groups on the surfaces of the chitosan films were blocked with 2% acetic anhydride in methanol solution for 1 h at room temperature. Then, the films were soaked in a 1 M sodium hydroxide solution for 1 h to neutralize the remaining acid. Thereafter, the films were washed thoroughly with distilled water. Succinic anhydride modified chitosan was labeled as SUC-CHI.

Step 2. The −COOH groups on the SUC-CHI were used to immobilize the GRGDS peptide. They were activated with a mixture of EDC/NHS. 5 mg/mL EDC and 5 mg/mL NHS in MES buffer solution (0.1 M, pH 6.5) was added, and the films were activated for 2 h at 4 °C. After the EDC/NHS solution was removed, different concentrations of the GRGDS peptide (20, 50, and 100 μg/mL; 0.3 mL in one well of 24-well tissue culture clusters or 1.6 mL in one 35-mm tissue culture plate, respectively) were added and incubated for 9 h at 4 °C. Finally, the films were rinsed with distilled water to remove any unreacted reagents. Unmodified chitosan film was used as negative control, labeled CHI. The other films were labeled 20-GRGDS, 50-GRGDS, and 100-GRGDS, according to the concentration of the GRGDS peptide.

ESCA. The chemical characteristics of the surface of the unmodified, succinic anhydride modified, and GRGDS-coupled chitosan films were investigated by ESCA (PHI-5300 ESCA; Philadelphia, U.S.A.). The ESCA spectrum was obtained with an aluminum anode (Al K_α = 1486.6 eV), and the survey scan range was 0−1000 eV. The base pressure of the analysis chamber was less than 10^{-7} Pa.

ATR-FTIR. Attenuated total reflection spectra of the unmodified, succinic anhydride modified, and GRGDS-coupled chitosan films were obtained with an FTIR spectrometer (PerkinElmer, Norwalk, CT).

AAA. Samples of GRGDS-coupled chitosan films were mixed with 4 mL of a 6 M HCl aqueous solution to hydrolyze the attached amino acids. The mixture was kept at 110 °C for 24 h and then dried in an oven at 70 °C for 4−5 days. Then, the hydrolyzed samples were analyzed with an amino acid analyzer (S-433D; SYKAM Co. Germany).

MC3T3-E1 Cell Culture. To study the biocompatibility of the unmodified and GRGDS-coupled chitosan films in bone formation, MC3T3-E1 cells (Japan Riken Cell Collection) were chosen to test the cytocompatibility of the materials. During the experiment, MC3T3-E1 cells were cultured in DMEM-10% FBS containing 100 U/mL penicillin and 100 μg/mL streptomycin. The cells were maintained in a humid, 5% CO_2 incubator and passaged using 0.25% trypsin. The culture medium was replaced every 2 days. Prior to cell culture experiments, the 24-well tissue culture clusters and 35-mm tissue culture plates precoated with unmodified and GRGDS-coupled chitosan films were sterilized by exposure to UV light (15-W UV sterilamp, Philips) for 30 min, followed by a rinsing step of 30-min rinse in sterile phosphate-buffered saline (PBS) solution.

Acquisition of Cell Images. The films permitted the use of light microscopy to study cell−material interactions in detail. The MC3T3-E1 cells were trypsinized from the culture flasks, washed once in medium, and then collected by centrifugation. The seeding density was adjusted to 5×10^4 cells/mL, and 1 mL of cell suspension was added to each well of the 24-well tissue culture clusters precoated with unmodified and GRGDS-coupled chitosan films. The cells were then allowed to attach to the films and remained undisturbed in a humidified incubator (37 °C and 5% CO_2) for 1 or 2 days. After incubation, the specimens were viewed using an inverted phase contrast microscope (Axiovert 10; Opton). Images from the microscope were acquired using a digital camera (C-5060; Olympus, Japan).

Cell Attachment. Cell attachment experiments were carried out in medium without serum. MC3T3-E1 cells were trypsinized from the culture flasks, washed once in the medium without serum, and then collected by centrifugation. The pellet containing the cells was then resuspended in medium without serum. The cell density was adjusted to 1×10^5 cells/mL. A 1-mL aliquot of cell suspension was added to each well of the 24-well tissue culture clusters precoated with unmodified and GRGDS-coupled chitosan films, and the cells were allowed to attach to the films undisturbed in a humidified incubator (37 °C and 5% CO_2) for 4 or 8 h. After incubation, the wells were rinsed twice with PBS, then 100 μL MTT (3-[4,5-dimethylthiazol-2-yl]-2,5-diphenyltetrasodiuim bromide, 5 mg/mL, Amresco0793) and 900 μL medium were added to each well and the samples were incubated at 37 °C for 4 h. The MTT solution was removed, and the remaining insoluble blue formazan crystal was dissolved in dimethyl sulfoxide (DMSO). A 100-μL aliquot of solution from each well was aspirated and poured into a 96-well plate for absorbance measurement. The absorbance was directly proportional to cell viability. The absorbance was measured at 570 nm using an ELISA reader (model 550; BioRad).

Competitive Binding Study. The specific interaction between the GRGDS-coupled surfaces and the MC3T3-E1 cells was assessed via a competitive binding experiment using soluble GRGDS peptides as previously described.[27] Briefly, soluble peptide solutions (20, 50, 100 μg/mL) were prepared using medium without serum and then filtered using a PES membrane filter (0.22 μm pore diameter, MILLIPORE, Ireland) for sterilization. MC3T3-E1 cells were enzymatically using trypsin solution and resuspended in medium without serum at 1.0×10^5 cells/mL. 1 mL of cell suspension and 0.3 mL soluble peptide solution were mixed in a 4.5 mL sterile centrifuge tube. The resulting cell suspension was incubated for 10 min, seeded on the 20-GRGDS materials, then cultured for 4 h under standard culture conditions. After 4 h, the cells on the films were rinsed with PBS twice and measured by MTT assay. 20, 20+20S, 20+50S and 20+100S represent 20-GRGDS and 20-GRGDS with 20, 50, and 100 μg/mL soluble GRGDS peptides, respectively.

Cell Proliferation. The cell proliferation experiment was carried out in medium containing 10% fetal bovine serum. The cell density was adjusted to 5×10^4 cells/mL. A 1-mL aliquot of cell suspension was added to each well, and the cells were allowed to attach to the films in a humidified incubator (37 °C and 5% CO_2) for 1, 4, or 7 days. The culture medium was replaced every 2 days. After incubation, the wells were rinsed twice with PBS, then 100 μL MTT and 900 μL medium were added to each well and incubated at 37 °C for 4 h. As before, the MTT solution was removed, and the insoluble blue formazan crystal was dissolved in DMSO. A 100-μL aliquot of solution from each well was aspirated and poured in a 96-well plate for absorbance measurement at 570 nm using an ELISA reader (model 550, BioRad).

Actin Localization. The cytoskeletal organization of the MC3T3-E1 cells was examined by selectively labeling F-actin microfilaments with a fluorescent, phallotoxin-conjugate probe, rhodamine phalloidin. MC3T3-E1 cells were seeded with a density of 4×10^4 cells/mL. A 2-mL aliquot of cell suspension was added to each 35-mm tissue culture plate precoated with unmodified and GRGDS-coupled chitosan films for 2 days in medium containing 10% fetal bovine serum at 37 °C. After incubation, cells were washed twice with prewarmed PBS. Then, the samples were fixed in 3.7% formaldehyde solution in PBS for 10 min at room temperature. After the samples were rinsed three times with PBS, 0.1% Triton X-100 in PBS was added to extract for 3−5 min. After rinsing, 1% bovine serum albumin (BSA) was used to preincubate fixed cells for 30 min to reduce nonspecific background staining with fluorescent phallotoxins. Then, the cells were stained with 0.165 μM rhodamine phalloidin (Molecular Probes) in the dark at room temperature for 20 min. After incubation, the tissue culture plates were washed with PBS several times and examined using an Olympus Fluoview confocal laser-scanning microscope (FV 500, Olympus, Japan) with a 60× objective.

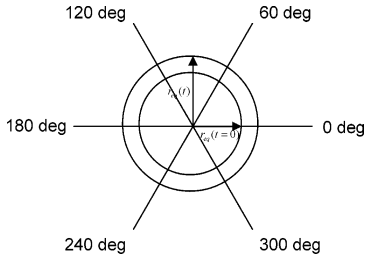

Figure 1. Schematic diagram of the megacolony migration assay, in which, first, $r_{eq}(t = 0)$ was calculated from the inner circle that was obtained from the line along the outermost front cells at day 0, and then, $r_{eq}(t = 3$ days) from the outer circle was calculated in the same manner at day 3 for the radially migrating cell population. Images were acquired at center and along each axis shown from center. The $r_{eq}(t)$ presented here was the mean value of six independent measurements from different angles (0°, 60°, 120°, 180°, 240°, and 300°).

Cell Migration. Sterilized unmodified and GRGDS-coupled chitosan films were precoated in 35-mm tissue culture plates. A glass annulus (11.5 mm in inner diameter, 15.5 mm in outer diameter, and 11.0 mm in height) was placed on the surface of materials, thereby creating a confined area on the film. MC3T3-E1 cells were enzymatically lifted from their plates using a trypsin solution and resuspended at seeding concentrations of 1.33×10^5 cells/mL. Then, 600 μL of the cell suspension was seeded onto the confined area of the films, and the cells were allowed to attach to the films for 24 h. After 24 h, the annulus was removed, the nonadherent cells were washed twice with PBS, and 3 mL of fresh media was added to each well. The time at which the annulus was removed was referred to as day 0. The area covered by each cell population was visualized and digitized using an inverted microscope (Axiovert 10, Opton) at an objective magnification of 10×. The microscope was used to quantify changes in cell density with increasing radius from the center of the initial cell population. To calculate changes in area of the main cell population, the radius was measured from the center of the circle to a point at the edge where the majority of the cell population had moved. The data presented were the mean values of six independent measurements from different angles (Figure 1: 0°, 60°, 120°, 180°, 240°, and 300°). Changes in cell density with radial distance were verified using images collected with a digital camera (C-5060; Olympus, Japan) at the center of the population and at specified radial positions from the center, as shown in Figure 1. After visualization of changes in cell density with radial distance, cells were allowed to migrate up to 3 days under standard culture conditions. The change in the radius of the cell megacolony was digitized every 24 h. Briefly, image analysis was performed as follows: The equivalent radius $r_{eq}(t)$ of the megacolony was meausued by splicing digital images together to form a composite image and then scaling the distance from the center of the circle to a point at the edge where the majority of the population had moved. The average migration distance $\langle d_c \rangle$ for MC3T3-E1 cells on different surfaces was calculated as follows:

$$\langle d_c \rangle = \frac{r_{eq}(t = 3 \text{ days}) - r_{eq}(t = 0)}{3} \quad (1)$$

and the megacolony area (A) of cells was computed by

$$A(t) = \pi r_{eq}(t)^2 \quad (2)$$

The change in the cell megacolony area $f(t)$ was quantified by the ratio

$$f(t) = \frac{A(t)}{A_0} \quad (3)$$

where $A(t)$ and A_0 are the areas of the megacolony at times t and $t = 0$, respectively.

Alkaline Phosphatase (ALP) Activity Assay. The cell differentiation assay was performed according to procedures reported by Yang et al.[28] In the differentiation stage, the culture medium was replaced with DMEM medium containing 10% FBS, 10 mM sodium β-glycerophosphate, and 50 μg/mL ascorbic acid. The culture medium was replaced every 2 days.

After culture in differentiation-inducing medium for 28 days, the medium was removed and the 24-well culture clusters were rinsed with PBS, then the cells were lysed with a solution containing 0.1% Triton X-100. A bicinchoninic acid (BCA) protein assay reagent (#23227, Pierce) was used to determine the total intracellular protein content. ALP activity was measured on the 28th day of culture in differentiation-inducing medium. The medium was first removed and the culture clusters were rinsed with PBS buffer solution, then the cells were lysed in 0.5% Triton X-100 PBS buffer solution (pH 7.6) containing 1 mM $MgCl_2 \cdot 6H_2O$ and 50 mM Tris. ALP activity was assayed by utilizing an alkaline phosphatase kit (Zhongsheng Beikong Bio-technology and Science Inc. China). Aliquots (20 μL) of the cell lysate were incubated with 1 mL of reaction solution (containing 350 mmol 2-amino-2-methyl-1-propanol, 2 mmol $MgCl_2$ and 16 mmol *p*-nitrophenyl phosphate) at 37 °C for 60 s. Through the reaction, *p*-nitrophenyl phosphate was converted to *p*-nitrophenol, and the absorbance at 405 nm was measured with an ELISA reader (model 550, BioRad) at 1, 2, and 3 min. The ALP activity was normalized using total intracellular protein synthesis and was expressed as U/g.

Mineralization. Calcium deposition is considered to be a terminal stage of osteoblast differentiation, which is initiated during matrix maturation and is slowly increased until the mineralized matrix forms a stable bony structure. On the 21st day of culture in differentiation-inducing medium, the cells cultured on the various materials were subjected to Von Kossa staining. The principle of Von Kossa staining is as follows: The cells are treated with a silver nitrate solution; calcium is then reduced by strong light and replaced with silver deposits, and can then be visualized as metallic silver. The medium was removed, and the culture clusters were rinsed with PBS buffer solution. Then, the clusters were fixed in 3.7% formaldehyde solution in PBS for 10 min at room temperature, washed with distilled water, and stained in 1% silver nitrate solution under UV light for 45 min. After being washed again with distilled water, the clusters were treated with 3% sodium thiosulfate for 5 min. Then, the clusters were counterstained with 1% neutral red for 1 min and washed with distilled water. The stained samples were then examined with an inverted phase contrast microscope (Axiovert 10, Opton). Images from the microscope were acquired using a digital camera (C-5060; Olympus, Japan).

Results and Discussion

ESCA Result. To investigate the details of the surface structural changes following each step of the modification procedure (Scheme 1), ESCA was employed because of its usefulness in obtaining information about the structure and chemical state of the surface of polymers. The peaks of ESCA wide spectra at 285, 400, and 532 eV were assigned to C1s, N1s, and O1s. The amount of C1s, N1s, and O1s calculated from the wide scan spectra for unmodified, succinic anhydride-modified, and GRGDS-coupled chitosan films is shown in Table 1. The surface of SUC-CHI showed a decrease from 5.20% to 4.70% in the percentage of N1s, while showing an increase in the percentages of C1s and O1s. This indicates that the reaction between chitosan and succinic anhydride mainly occurred on NH_2 moieties of chitosan. After the SUC-CHI was characterized,

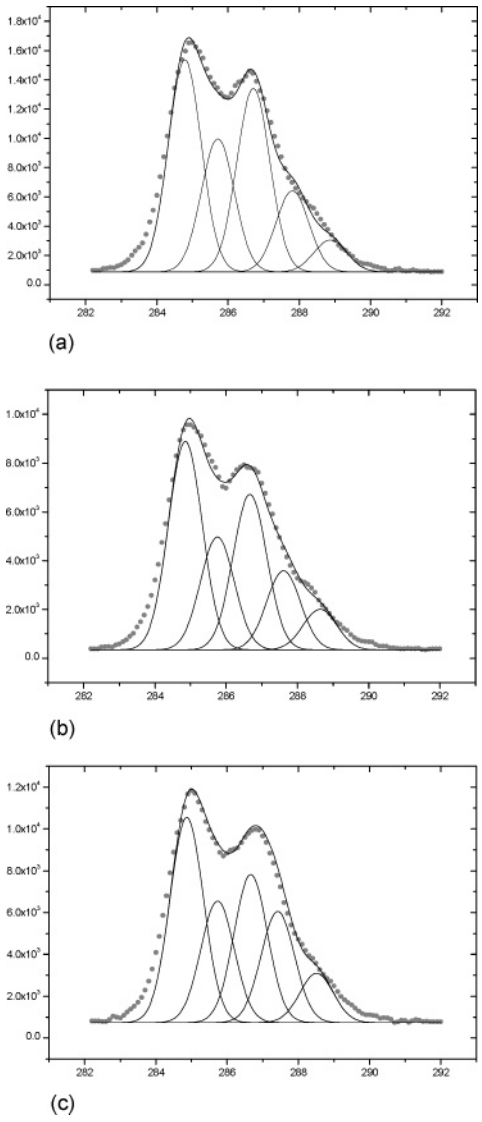

Figure 2. C1s spectra of chitosan and modified chitosan determined by XPS (*x*-axis, binding energy (eV); *y*-axis, intensity): (a) CHI; (b) SUC-CHI; (c) 100-GRGDS.

Table 1. Surface Elemental Compositions Calculated from the Wide Scan Spectra of ESCA

materials	C (%)	N (%)	O (%)	O/C	N/C
CHI	65.10	5.20	29.70	0.46	0.080
SUC−CHI	65.53	4.70	29.77	0.45	0.072
100-GRGDS	62.16	5.24	32.61	0.52	0.084

peptides (GRGDS) were immobilized onto the characterized surface. The N1s content of 100-GRGDS experienced an increase from 4.70% to 5.24% after peptide immobilization. Moreover, the O1s content of 100-GRGDS (32.61%) was larger than that of SUC-CHI (29.77%). The increase in N1s and O1s can be attributed to the grafting of GRGDS on the SUC-CHI surfaces. Increased N1s and O1s element content after RGD modification has been previously reported.[29−31]

Figure 2 shows the C1s spectra of unmodified and modified chitosan. The spectra were fitted using a combination of Gaussian and Lorentzian peak shapes so as to clarify the change in the chemical bonding of the C atom.[32,33] The C1s spectrum of different materials can be resolved into five components with different bonding states: the first at the energy of 285.0 eV assigned to C—C bond, the second at the energy of 285.8 eV

Table 2. Relative Peak Areas of the Fitted C1s Peaks of Surfaces of Chitosan and Modified Chitosan Films Obtained from ESCA Analysis

materials	peak 1: 285.0 eV (%) C−C	peak 2: 285.8 eV (%) C−NH_2	peak 3: 286.6 eV (%) C−OH	peak 4: 287.8 eV (%) O═C−NH_2	peak 5: 289.1 eV (%) O═C−OH
CHI	33.40	20.63	28.44	12.57	4.96
SUC−CHI	34.16	18.05	26.85	14.01	6.93
100-GRGDS	32.62	19.04	23.19	17.42	7.72

assigned to C−NH_2 bond, the third at the energy of 286.6 eV assigned to C−OH, the fourth at the energy of 287.8 eV assigned to O═C−NH_2, and the final at the energy of 289.1 eV assigned to O═C−OH. The corresponding relative peak areas of the fitted peaks were given in Table 2. The C1s spectrum of the different materials showed considerable changes in the chemical states of C. From Table 2 and Figure 2, it can be seen that the decrease of the peak areas of C−NH_2 bond and the increase of the peak areas of C−C, O═C−NH_2, and O═C−OH bonds after modification with succinic anhydride confirm the successful immobilization of short four-carbon arms on NH_2 moieties. After peptide coupling, the peak area of C−C was decreased (34.16% to 32.62%) in the presence of nitrogen-rich peptides, while O═C−NH_2 and O═C−OH bonds increased greatly. These changes can be attributed to the coupling of the GRGDS peptides. Thus, on the basis of ESCA results, it seems reasonable to say that GRGDS peptide grafting effectively takes place following the theoretical two-step scheme (Scheme 1).

ATR-FTIR Spectra. The two steps of immobilization of GRGDS on the chitosan through the use of a four-carbon arm were more precisely examined using attenuated total reflection (ATR)-Fourier transform infrared (FTIR) spectra. This technique has been proven to be a powerful tool for detecting amide bonds on solid surfaces.[34] The ATR-FTIR spectra of the unmodified and modified chitosan surfaces are shown in Figure 3. The typical spectrum of a chitosan film before any modification is represented by the black line in Figure 3. The ATR-FTIR spectrum begins to evolve as soon as the film is brought into contact with succinic anhydride, indicated by a rise in the intensity of the peak attributed to the carbonyl group (1718 cm^{-1}). This indicates the formation of a carbonyl group between chitosan and succinic anhydride. There is also a significant difference between SUC-CHI and GRGDS-modified chitosan. The peaks around 1312 and 1250 cm^{-1} can be attributed to the amide III band. Incorporation of GRGDS peptide led to small shifting in the spectrum of chitosan—the amide III band of CHI and SUC-CHI referred to 1260 and 1320 cm^{-1} peaks—but that of 50-GRGDS and 100-GRGDS shifted to 1250 and 1312 cm^{-1} peaks. In addition, the peak shapes of 50-GRGDS and 100-GRGDS were sharper than those of CHI and SUC-CHI. All these confirm that the short peptide GRGDS had been successfully immobilized on the surface of chitosan.

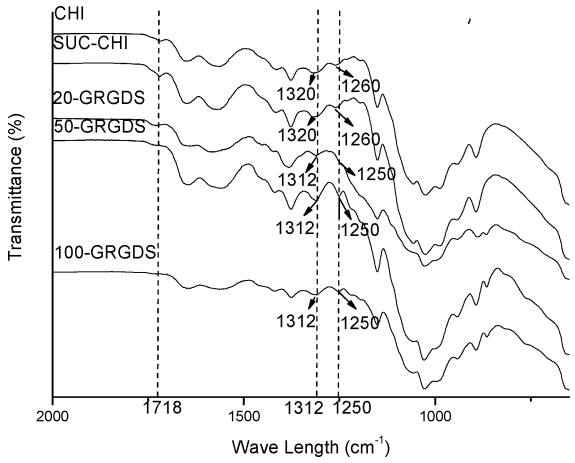

Figure 3. ATR-FTIR spectra of unmodified and modified chitosan films.

Table 3. Amounts of Immobilized GRGDS Peptides Per Unit Surface Area of Materials for Modified Chitosan Films

materials	20-GRGDS	50-GRGDS	100-GRGDS
density (nmol GRGDS/cm^2)	1.87	2.81	3.53

AAA Result. Quantitative analysis of the amount of GRGDS grafted on chitosan was performed by analyzing the amount of amino acids. For this analysis, there were four different immobilized amino acids, G, R, D, and S, which were hydrolyzed in 6 N HCl aqueous solution, and their concentrations in the hydrolyzing solution were determined using an amino acid analyzer (S-433D; SYKAM Co., Germany). The concentrations of Arg, Asp, and Ser were roughly the same, while the concentration of Gly was more than two times higher than that of the other three amino acids. The smallest value among those of Arg, Asp, and Ser was taken to be the peptide concentration. The amount of immobilized peptide per unit surface area of all films was determined, and the results are shown in Table 3. The immobilized peptide density of the surface was on the order of 10^{-9} mol/cm^2 (nmol/cm^2). The values for 20-GRGDS, 50-GRGDS, and 100-GRGDS were 1.87, 2.81, and 3.53 nmol/cm^2, respectively. Stemming from the early studies of RGD-mediated cell adhesion, there has been an ongoing discussion about how many RGD molecules are required to induce not only cell attachment but also cell spreading and focal contact formation. It has been reported that a minimal amount of 1 fmol RGD peptide/cm^2 was sufficient for cell spreading and as low as 10 fmol/cm^2 was sufficient for the formation of focal contacts and stress fibers on an RGD-functionalized glycophase glass surface.[35−37] As a general rule, a high RGD surface density is related to cell spreading, cell survival, focal contact formation, and to some extent proliferation. The results in Table 3 indicate that the surface density of the immobilized GRGDS was higher than the effective peptide density. Hence, the amount of immobilized GRGDS should be sufficient to affect cell attachment and the latter cell behavior like cell spreading and proliferation.

The results of ESCA, ATR-FTIR, and AAA confirm that the GRGDS peptide grafting effectively takes place following the theoretical two-step scheme (Scheme 1) and the surface density of immobilized GRGDS peptide is on the order of 10^{-9} mol/cm^2.

Acquisition of Cell Images. Micrographs of MC3T3-E1 cells cultured for 1 day on CHI and GRGDS-coupled chitosan films are shown in Figure 4a−d. The micrographs of a 1-day culture reflect the status of MC3T3-E1 cell attachment and spreading. On the CHI films, most cells retained a spherical shape and remained in suspension in the culture media. However, on

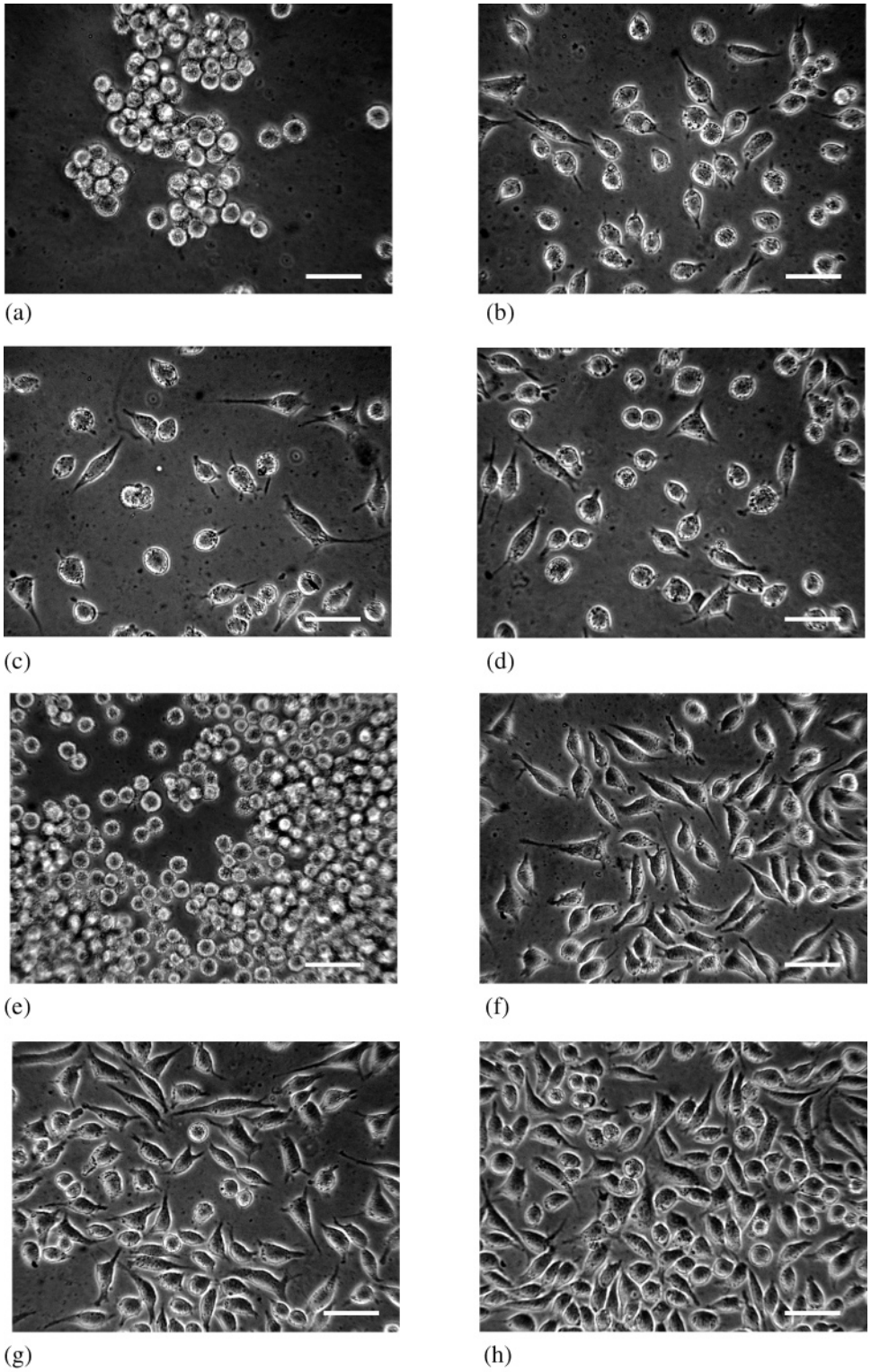

Figure 4. MC3T3-E1 cell morphology examined by inverted phase contrast microscope. The first day: (a) CHI; (b) 20-GRGDS; (c) 50-GRGDS; (d) 100-GRGDS. The second day: (e) CHI; (f) 20-GRGDS; (g) 50-GRGDS; (h) 100-GRGDS. Bar = 640 μm.

GRGDS-coupled chitosan films, a substantial number of cells changed from spherical to flat, assuming a fibroblast-like morphology, indicating that most cells had finished attachment and were in the process of spreading. Figure 4e−h also shows micrographs of MC3T3-E1 cells cultured for 2 days on the biomaterials. On the CHI films, there were still many round cells, because most spherical cells could not continue growing on the materials. However, on the GRGDS-coupled chitosan films, the number of flat-shaped cells increased, and the spreading was more uniform. The cells attached to the surface adopted an elongated shape. Spreading, which is an active process involving integrins, was optimal on the GRGDS-coupled chitosan and was reduced on unmodified chitosan.

Cell Attachment. It is reported that the RGD sequence can promote the attachment of cells because it is recognized by adhesion receptors on the cell membrane. Thus, the affinity of cells for materials should be improved with the immobilization of RGD, which can mimic the natural extracellular matrix. The

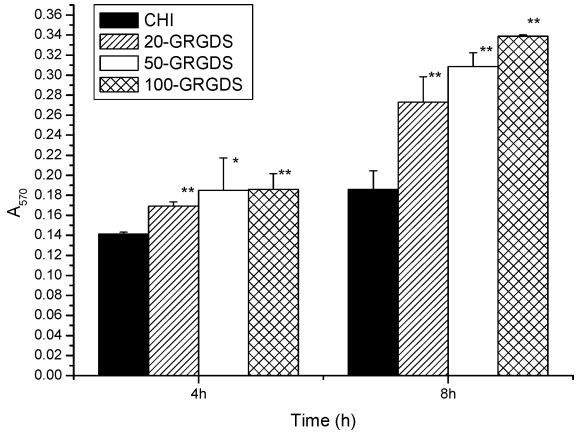

Figure 5. Attachment of MC3T3-E1 cells on the unmodified and GRGDS-coupled chitosan (initial seeding density was 1.0×10^5 cells/mL). $n = 4$. $^*P < 0.05$ relative to CHI. $^{**}P < 0.01$ relative to CHI.

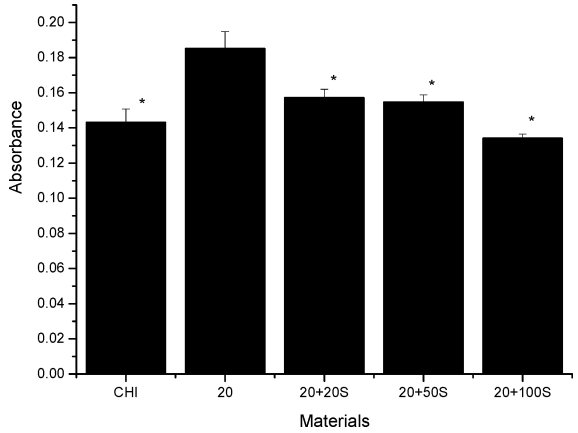

Figure 6. Competitive inhibition of attachment by soluble GRGDS peptides. MC3T3-E1 cells were incubated with soluble GRGDS peptides at three different concentrations (20, 50, 100 μg/mL; 0.3 mL) before seeding on 20-GRGDS (initial seeding density was 1.0×10^5 cells/mL; 1 mL). CHI was the negative control. $n = 4$. $^*P < 0.05$ relative to 20.

potential of GRGDS peptides to promote MC3T3-E1 cell attachment to biomaterials was investigated (Figure 5). MTT is a pale yellow substrate reduced by living cells to a dark blue formazan. Thus, an MTT assay was used to measure the attachment and proliferation of MC3T3-E1 cells. The attachment of cells increased with increasing incubation time for all materials. From Figure 5, it can be found that the attachment of cells on GRGDS-coupled chitosan surfaces was significantly higher than on the CHI surface 4 and 8 h after seeding. The attachment of MC3T3-E1 cells on GRGDS-coupled chitosan surfaces was dependent on the concentration of the peptide immobilized on the surface. These results indicate that GRGDS peptide was successfully incorporated onto the surface of chitosan films, presumably presenting a cell-binding domain, thereby allowing a specific binding with MC3T3-E1 cells.

To prove that the improved cell attachment was due to a biospecific interaction with GRGDS peptides on the surface, competitive inhibition of MC3T3-E1 cells attachment was investigated. Therein, cells were incubated with dissolved GRGDS with different concentrations before being seeded on CHI or 20-GRGDS surfaces. As shown in Figure 6, the number of adherent cells on 20-GRGDS was significantly greater than on CHI; however, the values were reduced when MC3T3-E1 cells were in the presence of soluble GRGDS peptides (20, 50, 100 μg/mL) over the entire range of concentrations prior to seeding. It is noticeable that the cell attachment on the surface of 20+100S was much less than that on the surface of CHI. This indicates that the biomimetic interaction between GRGDS-coupled chitosan and cells implicates specific binding events mediated by receptors that can be blocked by soluble GRGDS peptide and that the presence of GRGDS on the surface of chitosan plays a critical role in the attachment of cells on GRGDS-coupled chitosan.

Cell Proliferation. MTT assays on the first, fourth, and seventh day were used as a measure of relative cell proliferation. As shown in Figure 7, an increased absorbance on all surfaces at the end of the culture period showed that proliferation occurred on all films. MC3T3-E1 cell proliferation was significantly greater on GRGDS-coupled chitosan films than on CHI film after 4 or 7 days of culture. In particular, the number of cells on the 100-GRGDS film was the greatest, which correlates to the results for cell attachment on films. Successful cell attachment is beneficial to cell proliferation. The higher proliferation observed on the GRGDS-modified chitosan surface may suggest that the biomimetic surface modification was effective. Therefore, it can be concluded that the cell attachment

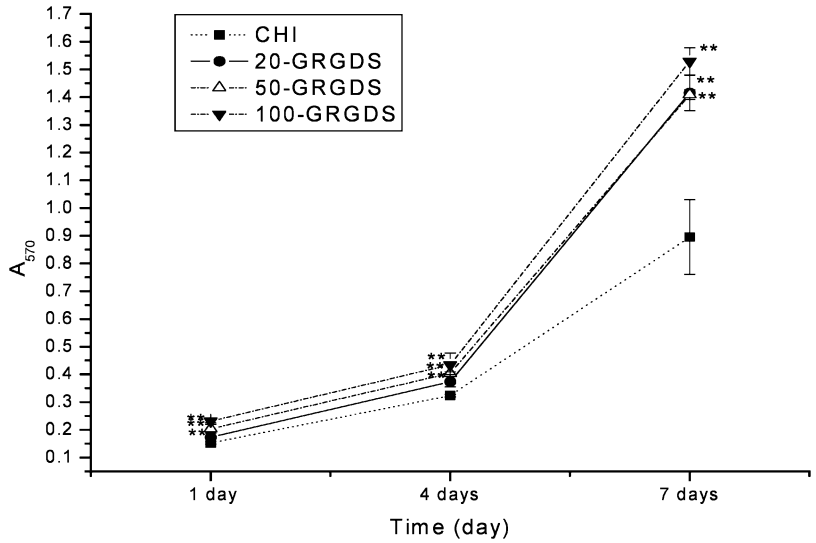

Figure 7. Proliferation of MC3T3-E1 cells on the unmodified and GRGDS-coupled chitosan (initial seeding density was 5.0×10^4 cells/mL; 1 mL). $n = 4$. $^{**}P < 0.01$ relative to CHI. (CHI, ■; 20-GRGDS, ◆; 50-GRGDS, △; 100-GRGDS, ▼.)

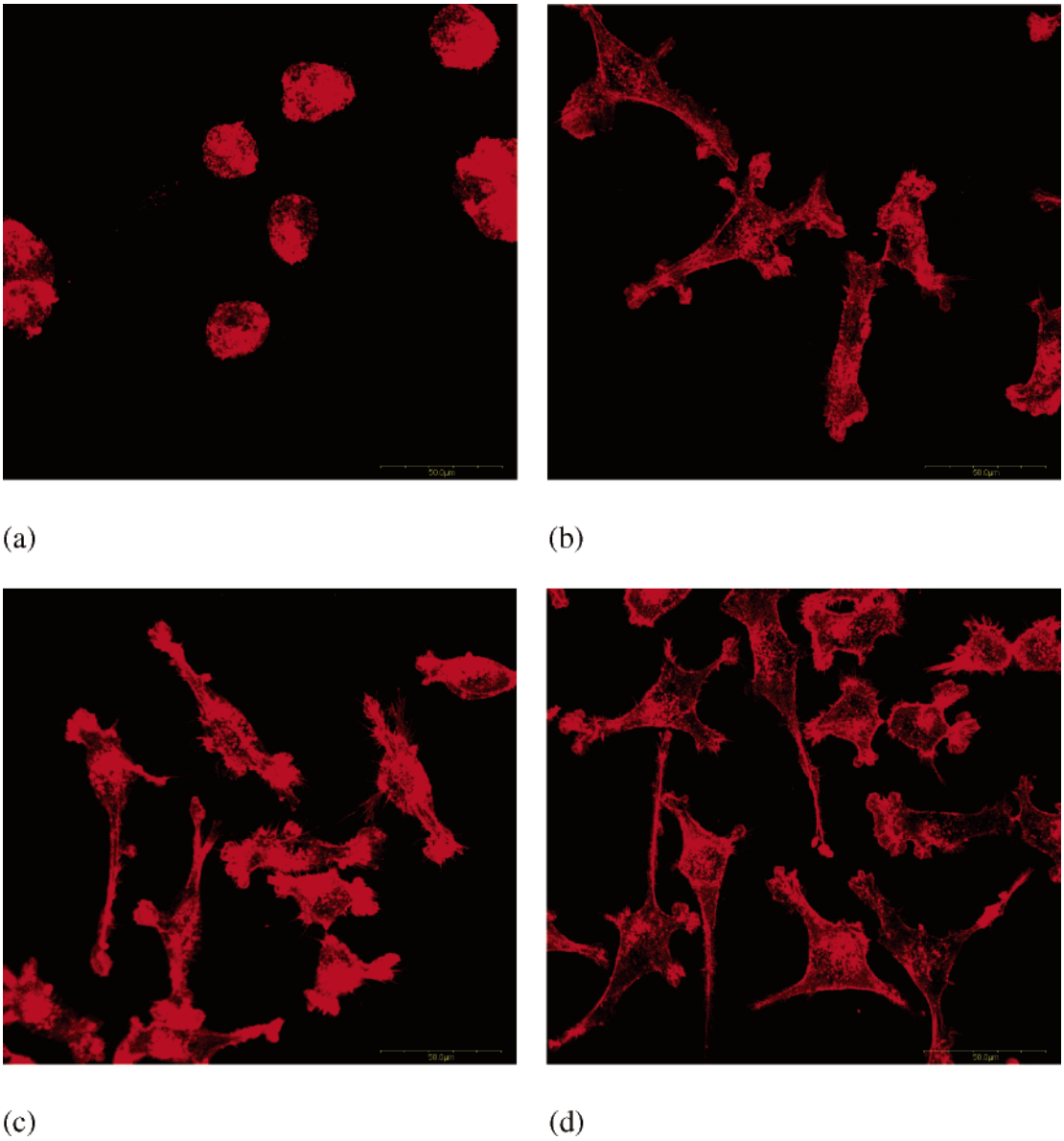

Figure 8. Actin cytoskeletal organization observed with fluorescent confocal microscopy of actin-stained MC3T3-E1 cells cultured for 48 h on (a) CHI, (b) 20-GRGDS, (c) 50-GRGDS, and (d) 100-GRGDS. Bar = 50 μm.

and proliferation on the surfaces of the biomaterials was significantly improved by GRGDS-sensitive cell-adhesion receptors.

Actin Cytoskeletal Organization. To further quantify the effect of the GRGDS sequence on osteoblast morphology, actin filament formation and organization was examined after 48 h of attachment. In this study, actin stress fibers were stained along with vinculin, a protein present in focal adhesions. Representative confocal images of actin staining of MC3T3-E1 cells attached to the various surfaces are shown in Figure 8. Cells grown on CHI showed a compact cell body, with little formation of cellular extensions. No organization of actin fibers was noted in the rounded MC3T3-E1 cells. However, cells on the 20-GRGDS, 50-GRGDS, and 100-GRGDS surfaces were fully spread and displayed robust cytoskeletal organization. Thin actin stress fibers were visible, and there were prominent focal contacts. The presence and arrangement of actin microfilaments and focal adhesion points help to indicate the degree of adhesion strength and are central to adhesion signaling.[38] Focal adhesions are micron-sized structures, usually located near the periphery of the cell, which form a strong adhesion to the substrate and secure bundles of actin microfilaments within the cell. They consist of a variety of proteins including vinculin and R-actinin, as well as signaling molecules such as focal adhesion kinase and paxillin.[39] Focal adhesion formation has important consequences for cell processes such as migration and differentiation.

Cell Migration. A fence-style assay was used to assess MC3T3-E1 cell migration on the unmodified and GRGDS-modified chitosan films. It was apparent that the MC3T3-E1 cells formed a sparsely populated rim adjacent to the outer migration front, while their megacolony became denser toward the center as shown in Figure 9. Figures 10 and 11 present the average migration distance $\langle d_c \rangle$ and the fractional increase of megacolony area $f(t)$ versus culture time for 3 days, respectively.

The average migration distance of MC3T3-E1 cell on GRGDS-modified chitosan was significantly higher than that on unmodified chitosan. When MC3T3-E1 cells were cultured on 100-GRGDS chitosan surface, $\langle d_c \rangle$ was 0.189 ± 0.016 mm/day; however, $\langle d_c \rangle$ was 0.073 ± 0.005 mm/day for unmodified chitosan surface. Similarly, the fractional increases of the megacolony area f (day 3) were 1.185 and 1.070 for 100-GRGDS chitosan surface and unmodified chitosan, respectively.

CDV

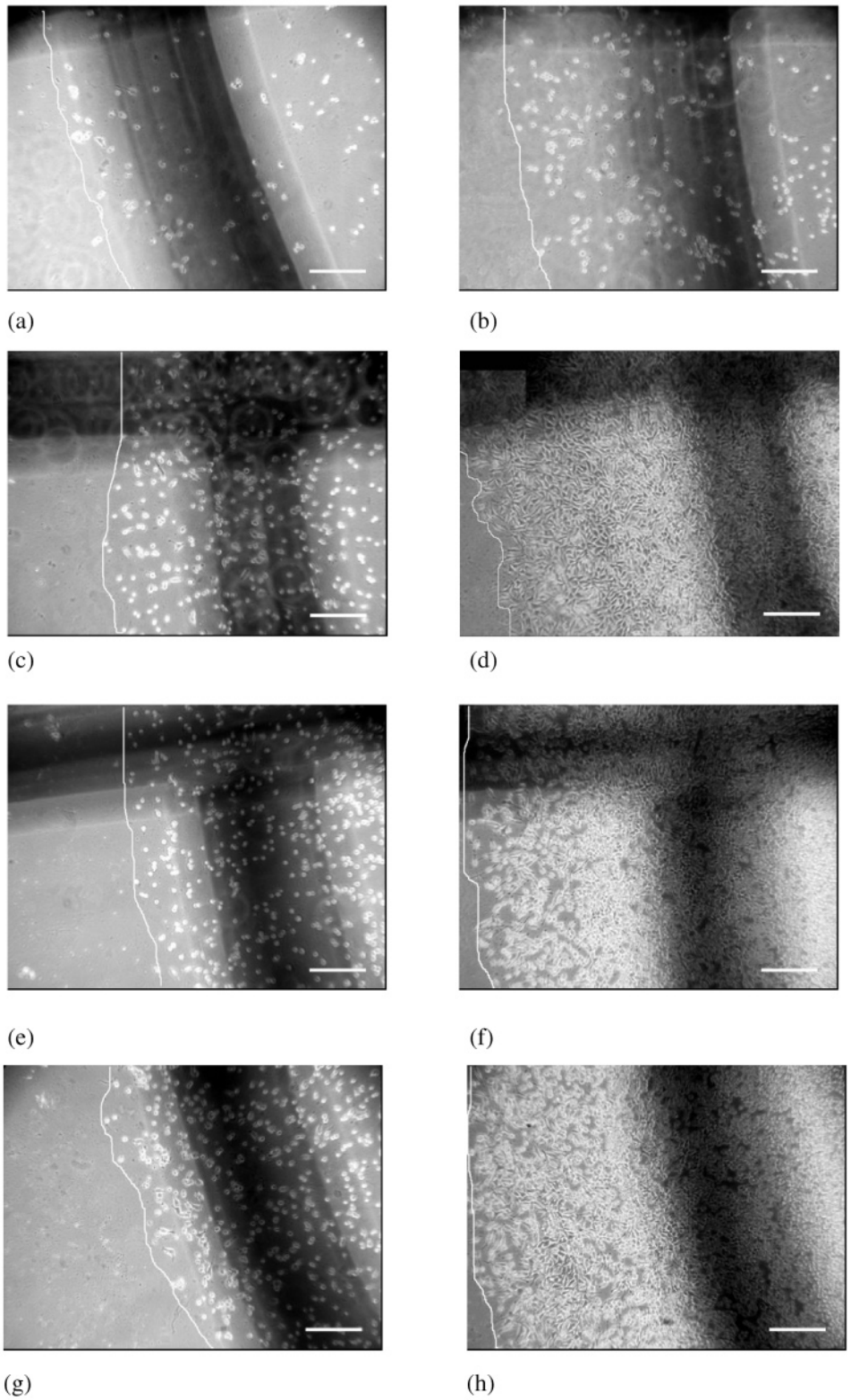

Figure 9. The leading edge of migration MC3T3-E1 cells at day 0 (a, c, e, g) and day 3 (b, d, f, h) on different materials: (a,b) unmodified chitosan; (c,d) 20-GRGDS; (e,f) 50-GRGDS; (g,h) 100-GRGDS. The solid lines were manually drawn along the outermost front of the motile cells. Bar = 200 μm.

Peptide concentration of GRGDS has an important role in MC3T3-E1 cell migration. When the peptide concentration was low (20-GRGDS), $\langle d_c \rangle$ was 0.134 ± 0.014 mm/day and f (day 3) was 1.128, whereas $\langle d_c \rangle$ was 0.147 ± 0.011 mm/day and f (day 3) was 1.141 when the peptide concentration was higher (50-GRGDS). The fractional increase of the MC3T3-E1 cell megacolony was relatively linear during the 3 days of culture.

Cell migration on biomaterials is desired for some applications, such as tissue ingrowth in tissue engineering scaffolds. The main functions of integrins in cell migration are assembly in focal adhesions at the front of the cell, mechanotransduction between the contractile forces of the cell and the underlying substrate while the cell body moves over, and the disassembly from focal contacts at the rear of the cell.[40−44] Some features

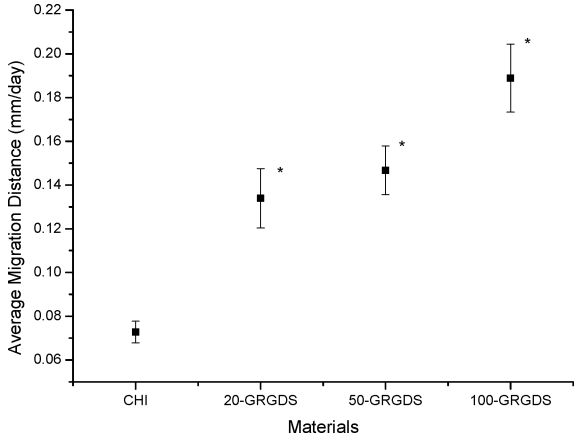

Figure 10. The average migration distance $\langle d_c \rangle$ of MC3T3-E1 on unmodified and GRGDS-coupled chitosan, which was calculated as the difference of the radii measured on day 0 and day 3 (eq 1). $n = 6$. $^*P < 0.05$ relative to CHI.

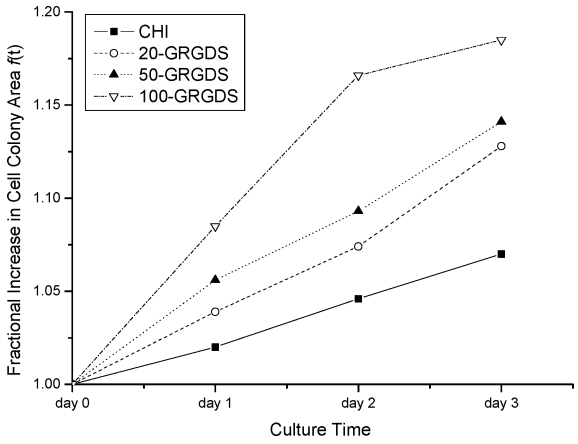

Figure 11. Fractional increase in cell megacolony area $f(t)$ of migrating MC3T3-E1 cells on unmodified and GRGDS-coupled chitosan (eqs 2 and 3).

of RGD-functionalized surfaces directly influence the functions of integrins in the migration process. First, the formation of focal contacts is necessary for cell migration. Therefore, higher GRGDS surface densities favor focal contact formation and promote cell migration. Second, blocking antibodies showed a predominant role of $\alpha_V\beta_3$ in cell migration on arterial walls.[45,46] GRGDS peptide has intermediate affinity to $\alpha_V\beta_3$. Therefore, selective GRGDS peptides would promote specific integrin migration. The migration of osteoprogenitor cells from a reservoir in the body to a bone defect is essential in that these cells contribute to the replacement and regeneration of bone tissue.[47]

ALP Activity. ALP is an early marker for osteoblast differentiation and an essential enzyme for ossification. The level of expression of this osteoblast phenotype depends on the stage of cellular differentiation. Figure 12 illustrates the changes in ALP activity of cells on the 28th day after culture in differentiation-inducing medium. By the 28th day, MC3T3-E1 cells on all materials presented significant ALP activity, which indicated the differentiation of MC3T3-E1 cells toward osteoblasts. In comparison with cultures on CHI, ALP activity for GRGDS-coupled chitosan was much higher. It should be noted that the ALP activity of MC3T3-E1 cells was dependent on the peptide concentration on the surface of GRGDS-coupled chitosan. These results indicate that immobilizing GRGDS peptide on chitosan may accelerate the differentiation of MC3T3-E1 cells into mature osteoblasts and such signaling peptide presented on the

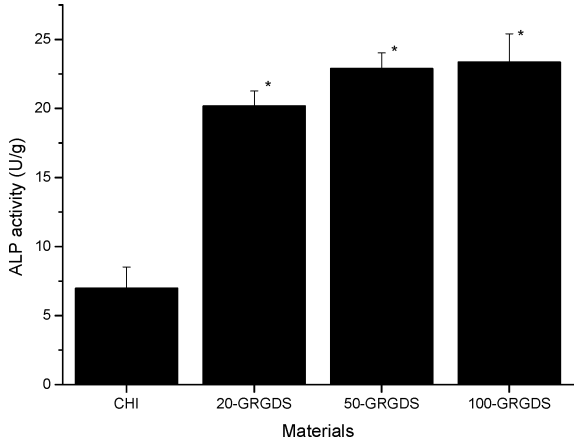

Figure 12. ALP activity of MC3T3-E1 cells on unmodified and GRGDS-coupled chitosan after being cultured in differentiation-inducing medium for 28 days. $n = 3$. $^*P < 0.05$ relative to CHI.

surface of chitosan provided sufficient biomolecular cues to promote early differentiation of MC3T3-E1 cells. ALP activity is the marker associated with ECM development and maturation of the osteoblast phenotypes, which has been routinely used as an early marker of osteoblast differentiation for in vitro experiments.[48] Our results imply that the biomimetic surface was involved not only in cell attachment but also in regulation of the cellular processes that generate a specific signal transduction cascade that enhances the differentiation of the osteoblasts.

Mineralization. The formation of calcium deposits is a late marker of osteoblast differentiation. The extent of mineralized ECM formed on unmodified and GRGDS-coupled chitosan surfaces examined by Von Kossa staining of surfaces following 3 weeks of incubation in differentiation medium is shown in Figure 13. Von Kossa staining stains mineral deposits brown to black. Consistent with the cell adhesion and proliferation results, the unmodified chitosan surface showed very low staining for mineralized matrix. However, enhanced mineralization was present in the surfaces with immobilized adhesive peptides, with the highest mineralization on the surfaces with the highest GRGDS concentration. These results are in accordance with the expression of the ALP activity, indicating that GRGDS peptide on the chitosan accelerated ECM mineralization. Rezania and Healy[49] reported a similar dependence of mineralization by osteoblasts on peptide density. In the case of the unmodified chitosan, the lower initial cell attachment most likely delayed the time for reaching confluence, which contributed to the lack of mineralization. Thus, these data suggest that covalent immobilization of surfaces with ligands containing the cell-binding domains found in extracellular matrix macromolecules offers an advantage in mediating matrix mineralization in vitro. It is possible that the initial engagement of cell surface receptors with the immobilized GRGDS sequence may have triggered signal transduction pathways, modulating long-term mineralization of the matrix. Potentially, the presence of adhesive peptides allows for a more natural environment for anchorage-dependent osteoblasts, and thus, mineral deposition by the osteoblasts is increased. The production of a mineralized matrix by these suspended osteoblasts is a significant result and indicates that these networks may find applications in bone regeneration.

Overall, the results of the ALP activity and mineralization assays suggest that the MC3T3-E1 cells underwent differentiation into osteoblasts following attachment on the GRGDS-coupled chitosan. Since the MC3T3-E1 cells were cultured in

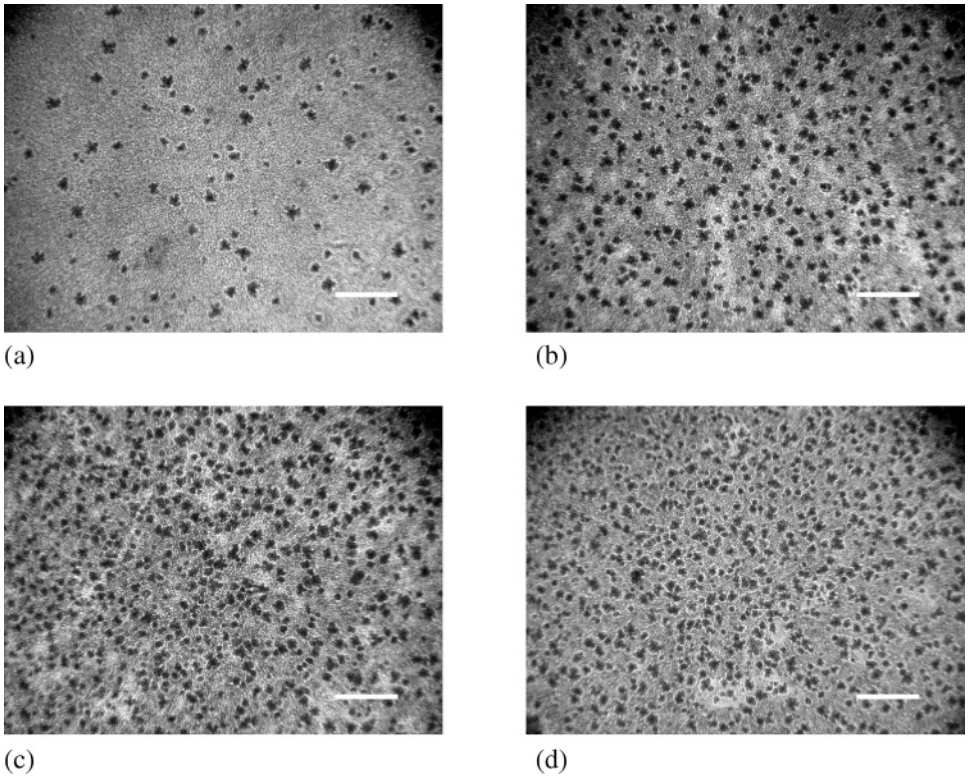

Figure 13. Von Kossa-stained MC3T3-E1 cells on unmodified and GRGDS-coupled chitosan after being cultured in differentiation-inducing medium for 21 days: (a) CHI; (b) 20-GRGDS; (c) 50-GRGDS; (d) 100-GRGDS. Bar = 400 μm.

the presence of osteogenic supplements, it is difficult to isolate the effect of the peptide presented by the materials compared to the soluble supplements in the media. However, it should be noted that there is an additive effect of the presentation of incorporated GRGDS pepetides. In addition, this effect of GRGDS peptide was concentration-dependent with higher peptide concentration-enhancing differentiation.

Conclusions

This study described a procedure for the modification of the surface of chitosan films with several concentrations of GRGDS, an osteoblast binding peptide, and characterized the immobilization of GRGDS peptide on the surface, as well as the MC3T3-E1 cell behavior on the modified surface. The results demonstrated that chitosan films can be successfully modified with GRGDS peptides, and the concentration of the immobilized GRGDS on the surface of chitosan was measured to be on the order of 10^{-9} mol/cm^2. In this study, large variations were observed in the cell behavior between unmodified and GRGDS-coupled chitosan materials. GRGDS immobilization enhanced attachment and proliferation of MC3T3-E1 cells on chitosan, which has been shown to be dependent on peptide concentration. Competitive inhibition of MC3T3-E1 cell attachment with soluble GRGDS peptides indicated that MC3T3-E1 cell adhesion was specifically mediated by GRGDS-sensitive cell adhesion receptor. The cytoskeletal organization of MC3T3-E1 cells was highly affected by the immobilization of GRGDS peptide on chitosan. The migration distance of MC3T3-E1 cells on the GRGDS-coupled surface was greater than the distance observed on unmodified chitosan. In addition, the migration of osteoblasts was enhanced with increasing peptide concentration. The GRGDS-coupled chitosan surface accelerated differentiation and mineralization of the MC3T3-E1 cells as evidenced by expression of ALP and calcium deposition. The ALP activity and calcium deposition were also affected by peptide concentration. These results indicate that optimization of peptide on the surface of chitosan presented here may be an effective method for modulating osteoblast function in scaffold-based bone tissue engineering.

Acknowledgment. The authors wish to thank the Tsinghua-Yue-Yuen Medical Science Fund and the National Basic Research Program (also called the "973" Program) of China (no. 2005CB623905) for supporting this research.

References and Notes

(1) Puleo, D. A.; Nanci, A. *Biomaterials* **1999**, *20*, 2311.
(2) Bauer, T. W.; Muschler, G. F. *Clin. Orthop. Relat. Res.* **2000**, *371*, 10.
(3) Shin, H.; Zygourakis, K.; Farach-Carson, M. C.; Yaszemski, M. J.; Mikos, A. G. *J. Biomed. Mater. Res., Part A* **2004**, *69A*, 535.
(4) Lane, J. M.; Tomin, E.; Bostrom, M. P. *Clin. Orthop. Relat. Res.* **1999**, *367S*, S107.
(5) Dee, K. C.; Bizios, R. *Biotechnol. Bioeng.* **1996**, *50*, 438.
(6) Anselme, K. *Biomaterials* **2000**, *21*, 667.
(7) Ruoslahti, E. *Annu. Rev. Cell. Dev. Biol.* **1996**, *12*, 697.
(8) Schaffner, P.; Dard, M. M. *Cell. Mol. Life Sci.* **2003**, *60*, 119.
(9) Hersel, U.; Dahmen, C.; Kessler, H. *Biomaterials* **2003**, *24*, 4385.
(10) Yang, X. B.; Roach, H. I.; Clarke, N. M. P.; Howdle, S. M.; Quirk, R.; Shakesheff, K. M.; Oreffo, R. O. C. *Bone* **2001**, *29*, 523.
(11) Kwunchit, O.; Bernd, W. M. *Int. J. Pharm.* **1997**, *156*, 229.
(12) Tokura, S.; Nishmura, S. I.; Sakairi, N.; Nishi, N. *Macromol. Symp.* **1996**, *101*, 389.
(13) Itoh, S.; Yamaguchi, I.; Shinomiya, K.; Tanaka, J. *Sci. Technol. Adv. Mater.* **2003**, *4*, 261.
(14) Xu, J.; McCarthy, S. P.; Gross, P. A. *Macromolecules* **1996**, *29*, 3436.
(15) Georgiev, I. L.; Illiev, I. G.; Asenova, M. K.; Kiril, F. *Water Res.* **2000**, *34*, 1503.
(16) Muzzarelli, R. A.; Mattioli-Belmonte, M.; Tietz, C.; Biagini, R.; Ferioli, G.; Brunelli, M. A.; Fini, M.; Giardino, R.; Ilari, P.; Biagini, G. *Biomaterials* **1994**, *15*, 1075.
(17) Mi, F. L.; Tan, Y. C.; Liang, H. F.; Sung, H. W. *Biomaterials* **2002**, *23*, 181.
(18) Cheng, M. Y.; Deng, J. G.; Yang, F.; Gong, Y. D.; Zhao, N. M.; Zhang, X. F. *Biomaterials* **2003**, *24*, 2871.

(19) Li, J.; Gong, Y. D.; Zhao, N. M.; Zhang, X. F. *J. Appl. Polym. Sci.* **2005**, *98*, 1016.
(20) Renbutsu, E.; Hirose, M.; Omura, Y.; Nakatsubo, F.; Okamura, Y.; Okamoto, Y.; Saimoto, H.; Shigemasa, Y.; Minami, S. *Biomacromolecules* **2005**, *6*, 2385.
(21) Chung, T. W.; Lu, Y. F.; Wang, H. Y.; Chen, W. P.; Wang, S. S.; Lin, Y. S.; Chu, S. H. *Artif. Organs* **2003**, *27*, 155.
(22) Ho, M. H.; Wang, D. M.; Hsieh, H. J.; Liu, H. C.; Hsien, T. Y.; Lai, J. Y.; Hou, L. T. *Biomaterials* **2005**, *26*, 3197.
(23) Craig, W. S.; Cheng, S.; Mullen, D. G.; Blevitt, J.; Pierschbacher, M. D. *Biopolymers* **1995**, *37*, 157.
(24) Beer, J. H.; Springer, K. T.; Coller, B. S. *Blood* **1992**, *79*, 117.
(25) Kantlehner, M.; Schaffner, P.; Finsinger, D.; Meyer, J.; Jonczyk, A.; Diefenbach, B.; Nies, B.; Holzemann, G.; Goodman, S. L.; Kessler, H. *Chembiochem* **2000**, *1*, 107.
(26) Pierschbacher, M. D.; Ruoslahti, E. *Nature (London)* **1984**, *309*, 30.
(27) Lieb, E.; Hacker, M.; Tessmar, J.; Kunz-Schughart, L. A.; Fiedler, J.; Dahmen, C.; Hersel, U.; Kessler, H.; Schulz, M. B. *Biomaterials* **2005**, *26*, 2333.
(28) Yang, M.; Zhu, S. S.; Chen, Y.; Chang, Z. J.; Chen, G. Q.; Gong, Y. D.; Zhao, N. M.; Zhang, X. F. *Biomaterials* **2004**, *25*, 1365.
(29) Lin, H. B.; Sun, W.; Mosher, D. F. Garciaecheverria, C.; Schaufelberger, K.; Lelkes, P. I.; Cooper, S. L. *J. Biomed. Mater. Res.* **1994**, *28*, 329.
(30) Sugawara, T.; Matsuda, T. *J. Biomed. Mater. Res.* **1995**, *29*, 1047.
(31) Wang, Y. H.; Hsu, J. J.; Lin, Y. S.; Lai, J. Y.; Chung, T. W. *J. Chin. Inst. Chem. Eng.* **2000**, *31*, 27.
(32) Zhang, D. M.; Cui, F. Z.; Luo, Z. S.; Lin, Y. B.; Zhao, K.; Chen, G. Q. *Surf. Coat. Technol.* **2000**, *131*, 350.
(33) Li, J.; Yun, H.; Gong, Y. D.; Zhao, N. M.; Zhang, X. F. *J. Biomed. Mater. Res., Part A* **2005**, *75A*, 985.
(34) Lin, Y. S.; Wang, S. S.; Chung, T. W.; Wang, Y. H.; Chiou, S. H.; Hsu, J. J.; Chou, N. K.; Hsieh, K. H.; Chu, S. H. *Artif. Organs* **2001**, *25*, 617.
(35) Massia, S. P.; Hubbell, J. A. *J. Cell Biol.* **1991**, *114*, 1089.
(36) Drumheller, P. D.; Elbert, D. E.; Hubbell, J. A. *Biotechnol. Bioeng.* **1993**, *43*, 772.
(37) Drumheller, P. D.; Hubbell, J. A. *Anal. Biochem.* **1994**, *222*, 380.
(38) Sastry, S. K.; Burridge, K. *Exp. Cell Res.* **2000**, *261*, 25.
(39) Geiger, B.; Bershadsky, A.; Pankov, R.; Yamada, K. M. *Nat. Rev. Mol. Cell Biol.* **2001**, *2*, 793.
(40) Horwitz, A. R.; Parsons, J. T. *Science* **1999**, *286*, 1102.
(41) Smilenov, L. B.; Mikhailov, A.; Pelham, R. J.; Marcantonio, E. E.; Gundersen, G. G. *Science* **1999**, *286*, 1172.
(42) Small, J. V.; Kaverina, I.; Krylyshkina, O.; Rottner, K. *FEBS Lett.* **1999**, *452*, 96.
(43) Beningo, K. A.; Dembo, M.; Kaverina, I.; Small, J. V.; Wang, Y. L. *J. Cell Biol.* **2001**, *153*, 881.
(44) Sheetz, M. P.; Felsenfeld, D.; Galbraith, C. G.; Choquet, D. *Biochem. Soc. Symp.* **1999**, *65*, 233.
(45) Slepian, M. J.; Massia, S. P.; Dehdashti, B.; Fritz, A.; Whitesell, L. *Circulation* **1998**, *97*, 1818.
(46) Clyman, R. I.; Mauray, F.; Kramer, R. H. *Exp. Cell Res.* **1992**, *200*, 272.
(47) Aubin, J. E. *J. Cell. Biochem.* **1998**, *30*/*31*, 73.
(48) Bancroft, G. N.; Sikavitsast, V. I.; van den Dolder, J.; Sheffield, T. L.; Ambrose, C. G.; Jansen, J. A.; Mikos, A. G. *Proc. Natl. Acad. Sci. U.S.A.* **2002**, *99*, 12600.
(49) Rezania, A.; Healy, K. E. *J. Biomed. Mater. Res.* **2000**, *52*, 595.

BM050913R